Gastroenterology 2016;151:526–539

# BASIC AND TRANSLATIONAL—PANCREAS

## YAP1 and TAZ Control Pancreatic Cancer Initiation in Mice by Direct Up-regulation of JAK–STAT3 Signaling

Ralph Gruber,[1] Richard Panayiotou,[2] Emma Nye,[3] Bradley Spencer-Dene,[3] Gordon Stamp,[3] and Axel Behrens[1,4]

[1]Mammalian Genetics Laboratory; [2]Transcription Laboratory; [3]Experimental Histopathology, The Francis Crick Institute, Lincoln's Inn Fields Laboratory, London, UK; and [4]School of Medicine, King's College London, London, UK

**See Covering the Cover synopsis on page 380; see editorial on page 393.**

**BACKGROUND & AIMS:** Pancreatitis is the most important risk factor for pancreatic ductal adenocarcinoma (PDAC). Pancreatitis predisposes to PDAC because it induces a process of acinar cell reprogramming known as acinar-to-ductal metaplasia (ADM)—a precursor of pancreatic intraepithelial neoplasia lesions that can progress to PDAC. Mutations in KRAS are found at the earliest stages of pancreatic tumorigenesis, and it appears to be a gatekeeper to cancer progression. We investigated how mutations in KRAS cooperate with pancreatitis to promote pancreatic cancer progression in mice. **METHODS:** We generated mice carrying conditional alleles of *Yap1* and *Taz* and disrupted *Yap1* and *Taz* using a Cre-lox recombination strategy in adult mouse pancreatic acinar cells (Yap1fl/fl;Tazfl/fl;Ela1-CreERT2). We crossed these mice with LSL-KrasG12D mice, which express a constitutively active form of KRAS after Cre recombination. Pancreatic tumor initiation and progression were analyzed after chemically induced pancreatitis. We analyzed pancreatic tissues from patients with pancreatitis or PDAC by immunohistochemistry. **RESULTS:** Oncogenic activation of KRAS in normal, untransformed acinar cells in the pancreatic tissues of mice resulted in increased levels of pancreatitis-induced ADM. Expression of the constitutive active form of KRAS in this system led to activation of the transcriptional regulators YAP1 and TAZ; their function was required for pancreatitis-induced ADM in mice. The JAK–STAT3 pathway was a downstream effector of KRAS signaling via YAP1 and TAZ. YAP1 and TAZ directly mediated transcriptional activation of several genes in the JAK–STAT3 signaling pathway; this could be a mechanism by which acinar cells that express activated KRAS become susceptible to inflammation. **CONCLUSIONS:** We identified a mechanism by which oncogenic KRAS facilitates ADM and thereby generates the cells that initiate neoplastic progression. This process involves activation of YAP1 and TAZ in acinar cells, which up-regulate JAK–STAT3 signaling to promote development of PDAC in mice.

*Keywords:* PanINs; Pancreatic Cancer Progression; Mouse Model; Inflammation.

The most common and lethal tumor of the pancreas, pancreatic ductal adenocarcinoma (PDAC), exhibits the histologic morphology and marker expression of pancreatic duct cells. However, many of these tumors originate from the other major exocrine cell type, acinar cells, through a reprogramming process known as acinar-to-ductal metaplasia (ADM).[1] ADM is characterized by a change in marker expression: acinar cells positive for amylase also begin to express the ductal cell marker CK19. These poorly differentiated cells express the pancreatic progenitor cell markers Pdx1 and Nestin[2,3] and are important precursors of malignancy.[4] Pancreatic intraepithelial neoplasia (PanIN) lesions have a well-established histologic progression toward PDAC,[5] and can arise from ADM lesions.[1] ADM is the earliest pre-neoplastic lesion that predisposes to PDAC, making acinar-to-ductal reprogramming a crucial step in pancreatic cancer initiation.

*KRas* mutations are found in >90% of all PDAC cases[6] and they occur early, in low-grade pre-neoplastic lesions.[7,8] Although the importance of *KRas* mutation in the development of ADM, PanIN, and pancreatic tumors is well established,[9] the mechanisms by which oncogenic Ras leads to PDAC are not fully understood.

Pancreatitis is a well-known risk factor for PDAC development in humans. Patients with hereditary pancreatitis show a 50-fold increase in pancreatic cancer incidence.[10] In mouse models, both acute and chronic inflammation of the pancreas accelerate pancreatic cancer progression.[1,11] Pancreatitis can be induced experimentally by injection of caerulein, which induces acinar cell death and inflammation.[12] In caerulein-induced pancreatitis, inflammation induces acinar cells to reprogram to form ADM lesions,[11] which may be transient, or in the presence of a $KRas^{G12D}$ mutation, persistent.[13] Transforming growth factor–$\alpha$ (TGF$\alpha$) administration or overexpression also cooperates with $KRas^{G12D}$ to induce ADM in vitro.[3,14] Pancreatic inflammation facilitates tumorigenesis by inducing ADM.

Expression of oncogenic $KRas^{G12D}$ at endogenous levels in acinar cells triggers progression to pancreatic adenocarcinoma very inefficiently. Stronger transgenic expression of oncogenic Ras,[15] or additional oncogenic stimuli, such as

***Abbreviations used in this paper:*** **ADM, acinar-to-ductal metaplasia; CMV, cytomegalovirus; ES, embryonic stem cell; HBSS, Hank's balanced salt solution; IL, interleukin; PanIN, pancreatic intraepithelial neoplasia; PBS, phosphate-buffered saline; PDAC, pancreatic ductal adenocarcinoma; TGF$\alpha$, transforming growth factor–$\alpha$.**

**Most current article**


0016-5085/$36.00
http://dx.doi.org/10.1053/j.gastro.2016.05.006

mutant p53[16] or TGF$\alpha$ overexpression,[17] are required. Many of these additional stimuli directly or indirectly increase Ras activity, suggesting that a positive feedback loop amplifying oncogenic Ras signaling is required for PDAC progression.[18]

The reliance of established PDAC tumors on *KRas*$^{G12D}$ expression can be alleviated by up-regulation of the transcriptional regulator YAP1.[19] YAP1 has also been implicated in progression from PanIN to PDAC,[20] but its contribution at the reprogramming stage is unclear.

Here we show that *KRas* mutation sensitizes acinar cells to reprogramming by activating YAP1 and TAZ signaling, which in turn up-regulates components of the JAK–STAT3 pathway. This increases sensitivity to inflammatory stimuli, which induces widespread ADM among *KRas*-mutant acinar cells. Importantly, inhibiting *KRas*$^{G12D}$- and pancreatitis-induced reprogramming by inactivating YAP1/TAZ also prevents progression to PanIN, highlighting the importance of this mechanism for pancreatic cancer initiation.

## Materials and Methods

### Mouse Lines

For the generation of conditional *Yap1* and *Taz/Wwtr1* knockout mice, embryonic stem (ES) cell clones carrying the respective targeted alleles were obtained from the Knockout Mouse Project (KOMP) Repository (Yap1<tm1a(KOMP)Mbp>; ES clone E08) and the European Conditional Mouse Mutagenesis (EUCOMM) Program (Wwtr1<tm1a(EUCOMM)Wtsi>; ES clone A08). Targeted ES cell clones (agouti C57BL/6 parental cell line JM8A3.N1) were injected into blastocysts of C57BL/6 background to generate chimeric mice, which were then crossed with *Flpo*-expressing mice (Tg(CAG-Flpo)1Afst; C57BL/6 background)[21] to remove the neo-selection cassette and obtain mice carrying the conditional floxed alleles Yap1<tm1c(KOMP)Mbp> and Wwtr1<tm1c(EUCOMM)Wtsi> isogenic on C57BL/6. The *Flpo*-allele was bred out and mice were maintained on a C57BL/6 background. For genotyping and validation of knockout alleles, see Supplementary Figure 4 and Supplementary Materials and Methods.

The *Stat3*$^{fl/fl}$, *Pdx1-Cre*, *R26-LSL-YFP*, *LSL-KRas*$^{G12D}$, and *Ela1-Cre*$^{ERT2}$ mouse lines have been described (see Supplementary Materials and Methods).

### Acute Pancreatitis Induction

Acute pancreatitis in C57BL/6 mice was induced by 8 intraperitoneal injections of caerulein (Sigma-Aldrich, St Louis, MO) dissolved in phosphate-buffered saline (PBS) given at 1-hour intervals on 2 consecutive days at a dose of 50 $\mu$g/kg body weight per injection (high dose). Other strains received a similar treatment schedule except with 6 injections at a dose of 40 $\mu$g/kg body weight per injection (low dose). Control animals received injections of PBS only.

### Gene Set Enrichment Analysis

Gene set enrichment analysis was performed on the published transcription profile of C57BL/6 Jackson mice treated with caerulein or PBS[22] and on the transcription profile of mouse liver organoids overexpressing YAP1,[23] with the software developed by the Broad Institute of the Massachusetts Institute of Technology and Harvard University. The settings are listed in Supplementary Materials and Methods.

### Primary Acinar Cell Culture

Mice were sacrificed by cervical dislocation, the pancreas was dissected out and transferred to ice-cold Hank's balanced salt solution (HBSS) supplemented with penicillin/streptomycin (Sigma-Aldrich). Pancreata were cut into small pieces and digested with 2 mg/mL Collagenase P (Roche Diagnostics, Indianapolis, IN) in HBSS for 15 minutes at 37°C. Cells were washed 3 times with HBSS supplemented with 5% fetal bovine serum and then filtered through 500-$\mu$m and 105-$\mu$m nylon meshes (Spectrum Laboratories, Rancho Dominguez, CA). The cell suspension was layered on top of 30% fetal bovine serum in HBSS, centrifuged at 1000 rpm for 2 minutes and the cell pellet was resuspended in acinar cell culture medium ([Waymouth's medium; Life Technologies, Carlsbad, CA] supplemented with 1% fetal bovine serum, penicillin/streptomycin [Sigma-Aldrich], 1 $\mu$g/mL dexamethasone [Sigma-Aldrich] and 100 $\mu$g/mL soybean trypsin inhibitor [Sigma-Aldrich]). The cell suspension was then infected with adenoviruses either obtained from the University of Iowa Carver College of Medicine (Ad5-GFP and Ad5-Cre-GFP), at a concentration of $1.25 \times 10^7$ plaque-forming units/mL, or generated by cloning (Ad-GFP, Ad-GFP-YAP1-5SA, and Ad-GFP-TAZ-S89A), at a concentration of $5 \times 10^5$ plaque-forming units/mL. Acinar cells were incubated with adenoviruses for 1 hour at 37°C. Six-well tissue culture plates were coated with an 800 $\mu$L layer of collagen solution (4 mg/mL rat tail collagen; BD Biosciences, San Jose, CA), 10% 10× Waymouth's medium (Sigma-Aldrich) and 0.02 mol/L NaOH; Sigma-Aldrich). The cell suspension was mixed 1:1 with collagen solution and plated onto the collagen layer. The acinar cell/collagen mix was allowed to solidify for 1 hour at 37°C before adding medium. Medium was changed on day 1 and day 3 after the isolation. Quantifications were done on day 5 after isolation. To harvest the cells, the collagen matrix was digested with 1 mg/mL collagenase P (Roche Diagnostics) diluted in HBSS for 30 minutes at 37°C.

### Production of Recombinant Adenoviruses

The vectors harboring the coding sequences of the phosphorylation mutants of YAP1 (5SA) and TAZ (S89A), kindly provided by S. Piccolo, were used to subclone the YAP1 and TAZ complementary DNAs in the pAd-Track-cytomegalovirus (CMV) vector (Addgene, Cambridge, MA; #16405). This results in the expression of YAP1/TAZ under the control of the CMV promoter and pAd-Track-CMV empty vector was used as control. The pAd-Track-CMV contains a GFP complementary DNA under control of a second CMV promoter. Recombinant adenoviruses expressing GFP, YAP1-5SA in combination with GFP or TAZ-S89A in combination with GFP were generated following the protocol as described.[24] Briefly, human HEK293A cells were co-transfected with pAd-Easy-1 (Addgene #16400) together with pAd-Track-CMV, pAd-Track-CMV-YAP1-5SA, or pAd-Track-CMV-TAZ-S89A. Adenoviruses were harvested 14 days after transfection. To generate higher viral titer, fresh HEK293A were infected with the adenoviruses and grown for 7 days before harvesting and this process was repeated 3 times.

Adenoviruses were purified using the Adeno-X Maxi Purification Kit (TaKaRa Clontech, Mountain View, CA) according to the manufacturer's protocol. Virus titers were determined by infecting HEK293T cells with a dilution series of the adenoviruses. After infection, cells were overlaid with agarose and plaques were visualized by MTT (Sigma-Aldrich) and quantified 7 days later. This protocol generated virus titer ranging from 1 to 6 $\times$ $10^8$ plaque-forming units/mL.

### Immunoblot Analysis and Ras-GTP Pulldown Assay

Protein lysates were obtained from dissected pancreata, primary acinar cells or PANC1 cells and homogenized in Cell Lysis Buffer (Cell Signaling, Danvers, MA) containing proteasome inhibitor (Sigma-Aldrich). Immunoblots were performed as described.[25] Polyvinylidene difluoride membranes (GE Healthcare, Little Chalfont, Buckinghamshire, United Kingdom) were incubated with antibodies against YAP1 (Cell Signaling; #4912 and Santa Cruz Biotechnology, Santa Cruz, CA; sc-15407); p-YAP1 (Ser127 in humans and Ser112 in mice; Cell Signaling; #4911); TAZ (Sigma-Aldrich; HPA007415); CK19 (DHSB; TROMA-III); STAT3 (Cell Signaling; #4904); p-STAT3 (Tyr705; Cell Signaling; #9131); LATS1 (Cell Signaling; #3477); p-LATS1 (Ser909; Cell Signaling; #9157); LIFR (Santa Cruz Biotechnology; sc-659); PDX1 (R&D Systems, Minneapolis, MN; MAB2419); SOX9 (Millipore, Billerica, MA; AB5535); p-Erk1/2 (Thr202/Tyr204; Cell Signaling; #9106); Erk1/2 (Cell Signaling, #9102); glyceraldehyde-3-phosphate dehydrogenase (Abcam, Cambridge, MA; ab9485); and ACTIN (Abcam; ab49900). Active Ras levels were determined by Ras-GTP pull-down assay (ThermoFisher Scientific, Logan, UT) using the Raf Ras-binding-domain fused to GST (Raf-RBD-GST) according to the manufacturer's instructions. Signal intensities of bands were quantified using ImageJ software.

### Statistics

Statistical analysis was performed using GraphPad Prism 6.0a software (GraphPad, La Jolla, CA) and 2-tailed Student *t* tests were used to generate *P* values. Normalized enrichment scores and nominal *P* values for the gene set enrichment analysis were generated using the software developed by the Broad Institute of the Massachusetts Institute of Technology and Harvard University. $P < .05$ was considered significant.

### Study Approval

Mouse experiments were carried out with the approval of the London Research Institute's Ethical Review Committee according to the UK Animals (Scientific Procedures) Act 1986.

## Results

### YAP1 and TAZ Are Up-Regulated in Pancreatitis

ADM caused by pancreatitis is an initiating step in pancreatic tumor development.[1] To find molecular regulators of this process, we performed gene set enrichment analysis[26] on the published transcriptional profile of mouse pancreata treated with caerulein[22] to identify pathways up-regulated in pancreatitis (Supplementary Figure 1*A*). Many of these pathways, such as Wnt, Notch, and JAK–STAT3, have previously been implicated in either acinar cell regeneration or in inducing ADM upon injury.[13,27–29] Intriguingly, the highest gene set enrichment scores were for YAP1 target genes (Figure 1*A* and Supplementary Figure 1*A*).

To investigate a possible role for YAP1/TAZ signaling in pancreatitis-induced ADM, we treated C57BL/6 mice with caerulein to induce pancreatitis (Figure 1*B*). In untreated mice, YAP1 and TAZ proteins showed nuclear localization in duct cells of the pancreas, with low or absent expression in acinar cells and islet cells[20,30] (Supplementary Figure 1*B*). Consistent with the gene set enrichment analysis, the YAP1/TAZ target genes *Ctgf*, *Cyr61*, *Ankrd1*, and *Amotl2* were overexpressed in caerulein-treated animals compared with control PBS-treated mice (Figure 1*C*). Caerulein treatment reduced activatory phosphorylation of the YAP1/TAZ inhibitory kinase Lats1 (Figure 1*D* and Supplementary Figure 2*A* and *B*). In line with this, we observed increased YAP1 and TAZ protein levels (Figure 1*D* and Supplementary Figure 2*A* and *B*), accompanied by strong nuclear localization, indicating more active YAP1/TAZ in caerulein-treated animals (Figure 1*E*). Levels of the duct cell marker CK19 were also increased, consistent with acinar-to-ductal reprogramming (Figure 1*D* and Supplementary Figure 2*A* and *B*). To determine the identity of the YAP1/TAZ-responsive cells, we performed immunofluorescence co-staining with pancreatic cell type specific markers. Cells coexpressing CK19 and the acinar cell marker amylase showed high levels of nuclear YAP1 and TAZ, with some stromal cells also positive (Figure 1*F*). Thus, YAP1/TAZ activity is elevated in the injured, inflamed pancreas, particularly in the subset of cells undergoing ADM.

### YAP and TAZ Are Up-Regulated in Acinar-to-Ductal Metaplasia Lesions Induced by $KRas^{G12D}$

We next asked whether YAP1/TAZ up-regulation is restricted to caerulein-induced ADM or also occurs during ADM induced by oncogenic Ras. The pancreatic tumor mouse model *LSL-KRas$^{G12D}$;Pdx1-Cre* develops PDAC with long latency and displays the whole spectrum of pre-neoplastic lesions[31] (Figure 2*A*). We found a strong signal for both YAP1 and TAZ in ADM lesions of these mice, and an up-regulation of YAP1 and TAZ in pancreatic protein lysates (Figure 2*A* and *B* and Supplementary Figure 3*A* and *B*). Analysis of YAP1 and TAZ immunostaining on human pancreatic tissue microarrays showed strong up-regulation of YAP1 in human ADM and PanIN pre-neoplastic lesions compared with normal acini (Figure 2*C*–*E*). TAZ was strongly up-regulated in ADM and to a lesser extent in PanIN lesions in mouse models and human tissues (Figure 2*A* and *C*–*E*). Surprisingly, we found a significant down-regulation of YAP1 and TAZ protein levels in human PDAC samples compared with ADM lesions (Figure 2*C*–*E*), suggesting a functional role of YAP1 and TAZ particularly during tumor initiation.

### YAP1 and TAZ Are Necessary and Sufficient for Acinar-to-Ductal Metaplasia Induction

To determine the functional requirement for YAP1/TAZ signaling in acinar-to-ductal reprogramming, we generated

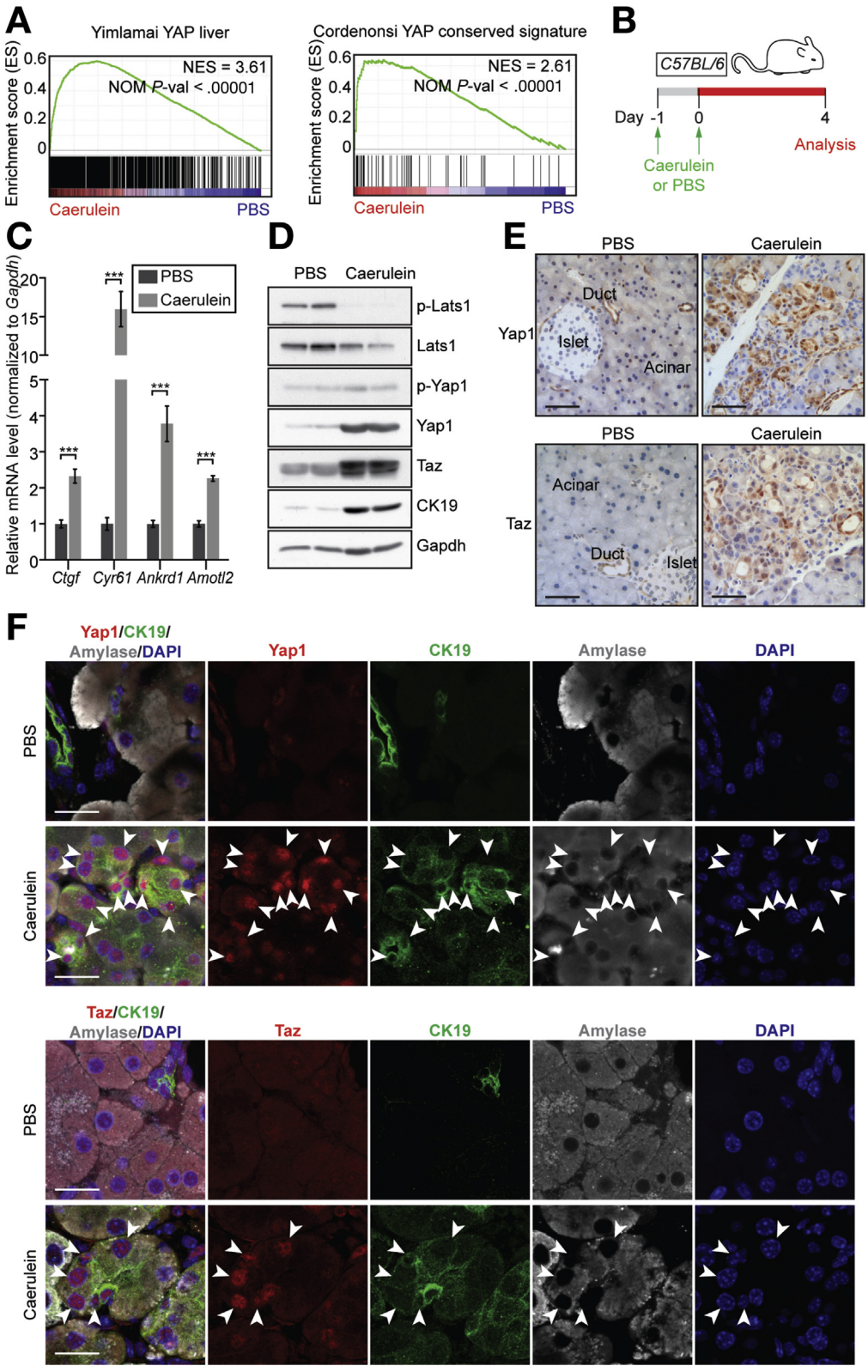


**Figure 1.** YAP1 and TAZ are up-regulated in pancreatitis. (*A*) Gene set enrichment analysis of transcription data from caerulein-treated pancreata[22] identified enrichment of the conserved YAP1 signatures reported by Yimlamai et al[23] and Cordenonsi et al.[47] Normalized enrichment score (NES) and nominal (NOM) *P* values are shown. (*B*) Scheme showing model of caerulein-induced acute pancreatitis in C57BL/6 mice. (*C*) Quantitative reverse transcription polymerase chain reaction of YAP1/TAZ target genes in caerulein-treated vs PBS-treated pancreata. n = 3 mice each group; means ± SEM are shown; ***$P < .005$, Student *t* test. (*D*) Immunoblots of pancreas lysates from caerulein- and PBS-treated animals. p-Lats1, phosphorylated Lats1 (Ser909); p-Yap1, phosphorylated Yap1 (Ser112). (*E*) Immunohistochemical stains of YAP1 and TAZ in pancreata of caerulein- and PBS-treated mice. Scale bars = 50 μm. n = 5–7 mice analyzed. (*F*) Triple immunofluorescence of pancreata from caerulein- and PBS-treated animals showing the duct marker CK19, the acinar marker amylase and either YAP1 or TAZ. *Arrowheads* indicate ADM cells. Scale bars = 20 μm. n = 5–7 mice analyzed. DAPI, 4′,6-diamidino-2-phenylindole dihydrochloride.

conditional floxed alleles of both *Yap1* and *Taz* (Supplementary Figure 4*A*–*F*). YAP1 and TAZ were efficiently deleted in $Yap1^{fl/fl}$;$Taz^{fl/fl}$ primary acinar cells (Supplementary Figure 5*A* and *B*). We combined the floxed $Yap1^{fl/fl}$ and $Taz^{fl/fl}$ alleles with the Cre-inducible oncogenic *LSL-*$KRas^{G12D}$ allele, shown to induce ADM in cultured acinar cells,[14] and assayed ADM in vitro (Figure 3*A*). As expected, Cre-mediated activation of $KRas^{G12D}$ transformed acinar cell clusters into tubular duct-like structures (Figure 3*B*). Deletion of *Yap1* significantly reduced the ability of $KRas^{G12D}$ to induce

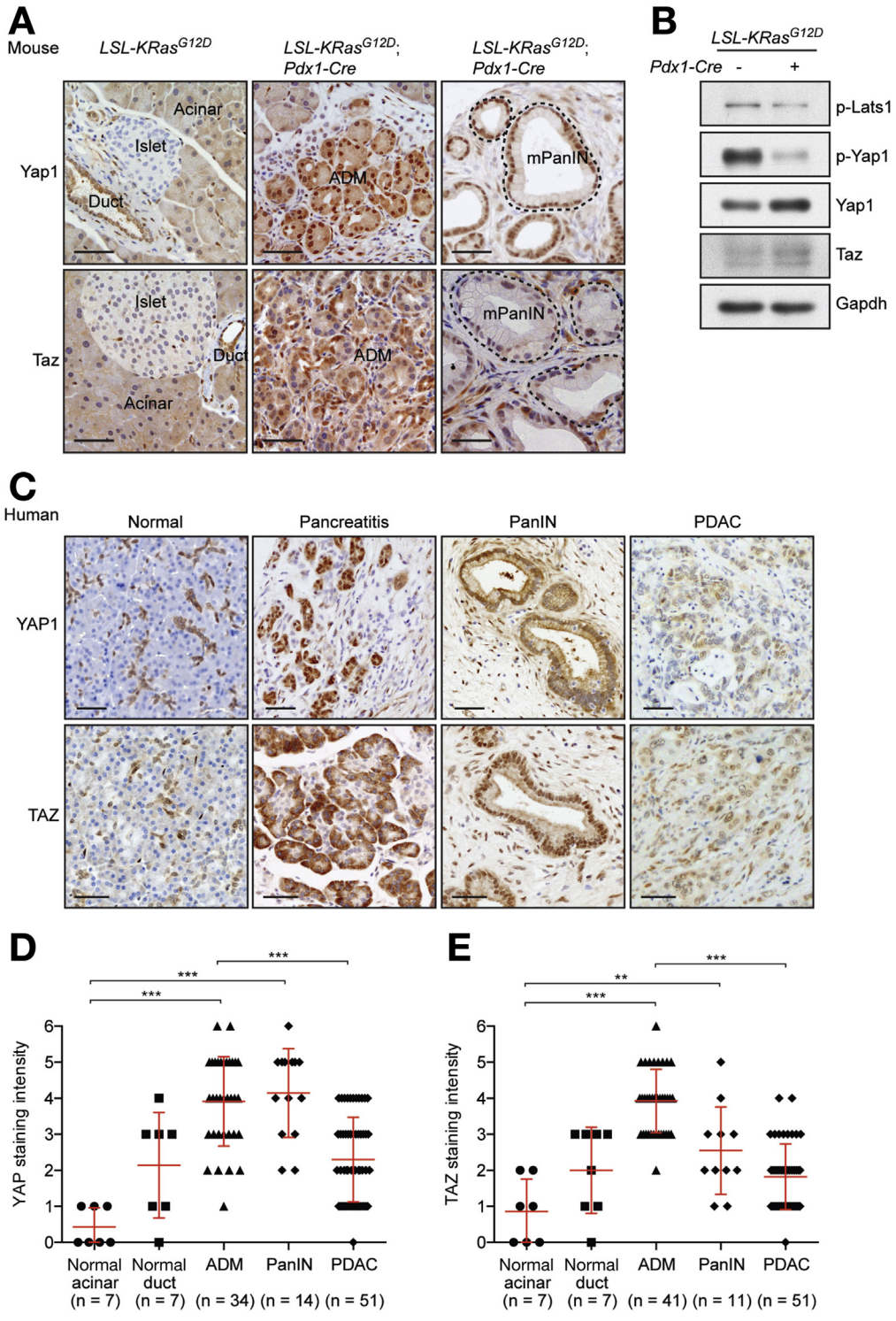


**Figure 2.** YAP1 and TAZ are up-regulated in ADM lesions induced by $KRas^{G12D}$. (*A*) Immunohistochemical analysis of YAP1 and TAZ in normal (*LSL-*$KRas^{G12D}$) pancreas and pancreas from 6-month-old *LSL-*$KRas^{G12D}$*;Pdx1-Cre* mice. Scale bars = 50 $\mu$m. *Dotted lines* highlight mouse PanIN lesions. n = 4–5 mice analyzed. (*B*) Immunoblot analysis of pancreas lysates from control *LSL-*$KRas^{G12D}$ and *LSL-*$KRas^{G12D}$*;Pdx1-Cre* mice. p-Lats1, phosphorylated Lats1 (Ser909); p-Yap1, phosphorylated Yap1 (Ser112). (*C*) Immunohistochemical analysis of YAP1 and TAZ on human pancreatic tissue microarrays. Scale bars = 50 $\mu$m. (*D, E*) Quantification of immunohistochemical staining intensity, ranging from absent (0) to highest (6) for YAP1 (*D*) and TAZ (*E*) on human pancreatic tissue microarrays. n = number of tissue cores. Means ± SD are shown. $^{**}P < .01$; $^{***}P < .005$, Student *t* test.

ADM, but deletion of *Taz* did not. However, in double-mutant *Yap1/Taz* acinar cells, $KRas^{G12D}$ failed to induce ADM (Figure 3*B* and Supplementary Figure 5*C* and *D*).

To address the requirement for YAP1 in vivo, we combined $Yap1^{fl/fl}$ with the *Pdx1-Cre* mouse line. Caerulein-induced ADM lesions co-expressing CK19 and amylase were readily observed in $Yap1^{fl/fl}$*;Pdx1-Cre* mice. However, these lesions were positive for YAP1 nuclear staining (Supplementary Figure 6*A*), suggesting that ADM occurred in cells that had escaped *Yap1* deletion. Consistent with this, polymerase chain reaction and immunoblot analysis showed that the recombination efficiency and consequent depletion of YAP1 was incomplete in $Yap1^{fl/fl}$*;Pdx1-Cre* mice (Supplementary Figure 6*B* and *C*). As an alternative model, we used a tamoxifen-inducible Cre line under the control of the acinar-specific *Ela1* promoter (*Ela1-*$Cre^{ERT2}$) in

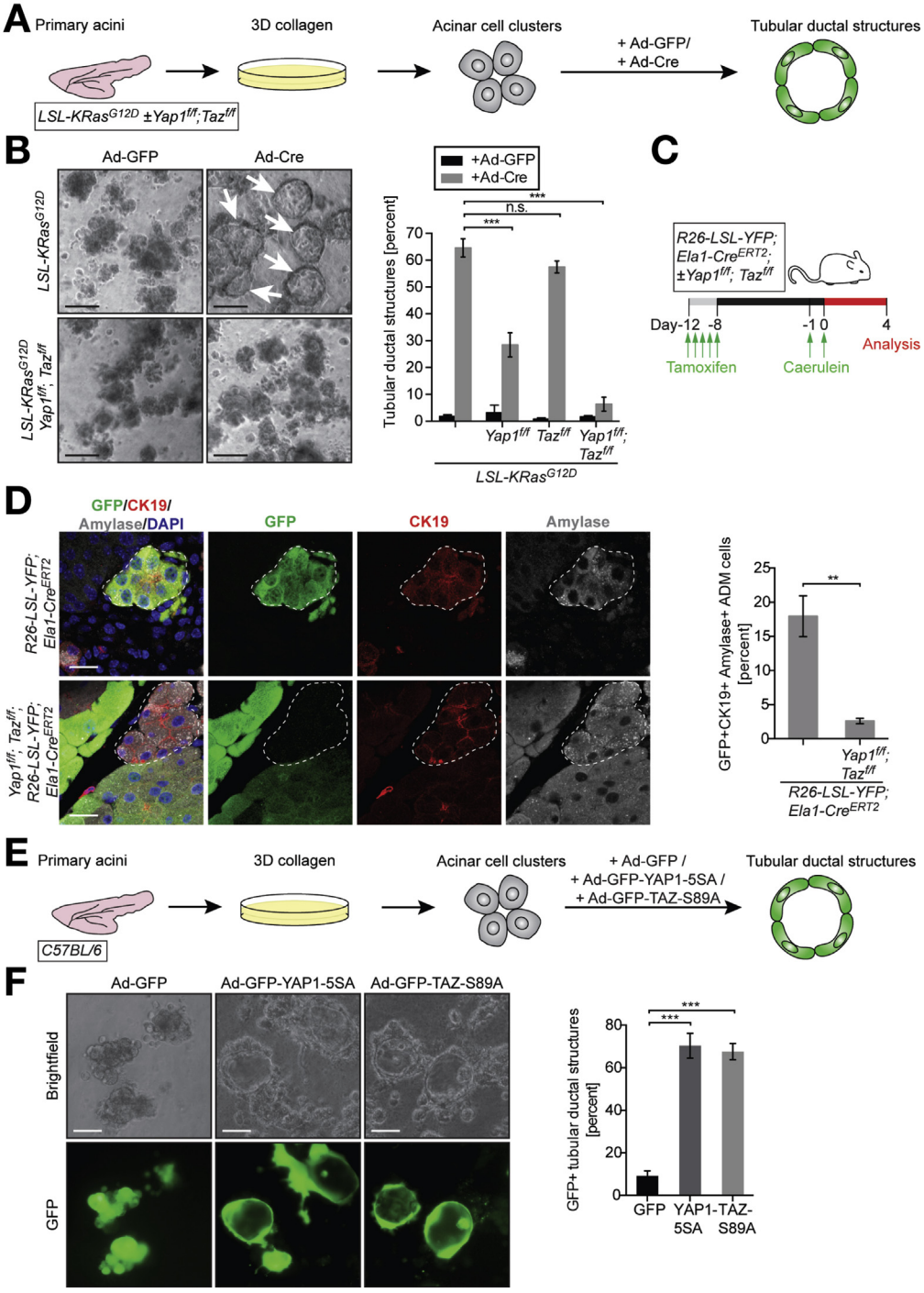


**Figure 3.** YAP1 and TAZ are necessary and sufficient for ADM induction. (*A*) Scheme showing in vitro assay for *KRas*$^{G12D}$-induced ADM. (*B*) Brightfield images of pancreatic acinar cell clusters on day 5 after isolation from *LSL-KRas*$^{G12D}$ and *LSL-KRas*$^{G12D}$*;Yap1*$^{fl/fl}$*;Taz*$^{fl/fl}$ mice. Cells were infected with adenoviruses encoding either GFP (Ad-GFP) or GFP plus Cre (Ad-Cre) on day 0. *White arrows*: tubular ductal structures. Scale bars = 50 $\mu$m. Quantification of tubular ductal structures of the indicated genotypes with n = 3–4 mice per group; means ± SEM are shown; ***$P < .005$, n.s., not significant, Student *t* test. (*C*) Experimental design of caerulein-induced acute pancreatitis in the acinar-specific and tamoxifen-inducible *Ela1-Cre*$^{ERT2}$ mouse model combined with the *R26-LSL-YFP* lineage tracer. (*D*) Triple immunofluorescence of pancreata from *R26-LSL-YFP;Ela1-Cre*$^{ERT2}$ and *R26-LSL-YFP;Yap1*$^{fl/fl}$*;Taz*$^{fl/fl}$*;Ela1-Cre*$^{ERT2}$ mice treated with caerulein as indicated in (*C*). Scale bars = 20 $\mu$m. *Dotted white lines* indicate ADM lesions. Quantification of GFP-positive ADM cells (CK19/amylase double-positive) as a percentage of total GFP-positive cells in caerulein-treated mice of the indicated genotypes. n = 3 mice per group; means ± SEM are shown; **$P < .01$, Student *t* test. (*E*) Scheme showing in vitro assay for YAP1 and TAZ-induced ADM. (*F*) Brightfield images (*upper panels*) and GFP signal (*lower panels*) of acinar cells after 5 days in culture, infected on day 0 with Ad-GFP, Ad-YAP1-5SA-GFP, or Ad-TAZ-S89A-GFP. Scale bars = 25 $\mu$m. Quantification of GFP-positive tubular ductal structures at day 5, in n = 3 experiments; means ± SEM are shown; ***$P < .005$, Student *t* test. DAPI, 4′,6-diamidino-2-phenylindole dihydrochloride.

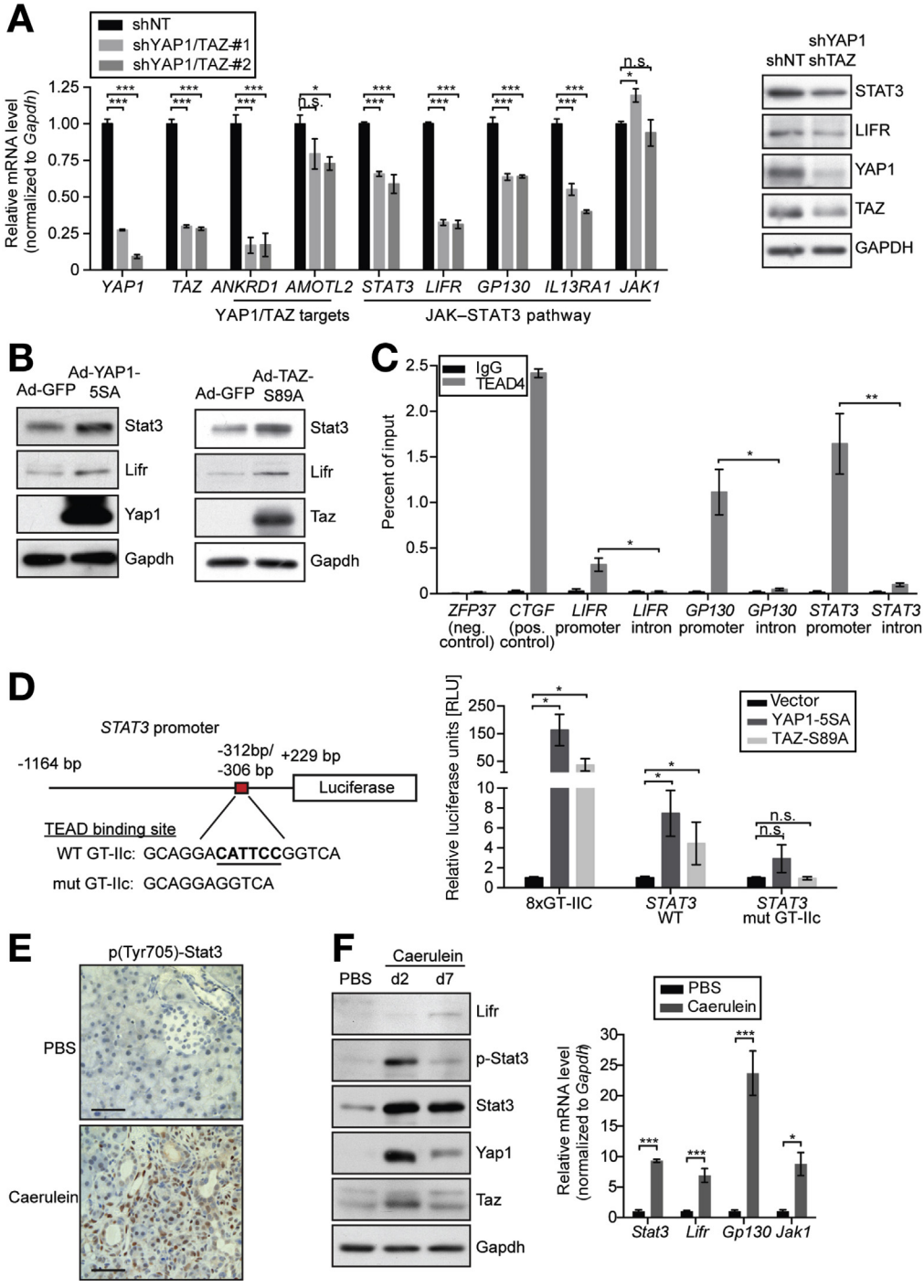


**Figure 4.** YAP1/TAZ activation controls JAK-STAT3 signaling via transcription of *STAT3*. (*A*) Quantitative reverse transcription polymerase chain reaction (RT-PCR) of the indicated genes and immunoblots of lysates from PANC1 cells expressing short-hairpin RNAs (shRNAs) against YAP1 and TAZ (shYAP/TAZ-#1 and -#2) or non-targeted shRNA control (shNT). n = 3; means ± SEM shown. (*B*) Immunoblots of primary acinar cell lysates 2 days after isolation and infection with Ad-GFP, Ad-YAP1-5SA-GFP, or Ad-TAZ-S89A-GFP. (*C*) Quantitative chromatin immunoprecipitation PCR of the *LIFR*, *GP130*, and *STAT3* loci (promoter and intron regions) using either IgG or an antibody against TEAD4. ZFP37 intron = negative control region; CTGF promoter = positive control region. n = 3 experiments; means ± SEM shown. (*D*) Scheme showing luciferase expression construct with human *STAT3* promoter region. Base pair (bp) numbers indicate position relative to *STAT3* transcription start site. *Red box* indicates GT-IIc TEAD binding motif; genomic sequence of WT GT-IIc shown below. Mutant *STAT3* promoter construct with a 6-bp deletion of the GT-IIc site (mut GT-IIc) was used as control. Luciferase expression analysis using wild-type and mutant *STAT3* promoter regions in AR42J acinar cells 1 day after transfection with empty vector, YAP1-5SA, or TAZ-S89A. An artificial TEAD luciferase reporter consisting of 8 GT-IIc motifs was used as positive control. n = 3–5 experiments; means ± SEM shown. (*E*) Immunohistochemistry showing phosphorylated STAT3 (Tyr705) in pancreata of caerulein- and PBS-treated C57BL/6 mice. Scale bars = 50 $\mu$m. n = 3 mice analyzed. (*F*) Immunoblots of pancreas lysates from PBS- and caerulein-treated animals on day 2 and day 7 after treatment. p-Stat3, phosphorylated Stat3 (Tyr705). Quantitative RT-PCR of JAK–STAT3 pathway genes in caerulein-treated vs PBS-treated pancreata 2 days after treatment. n = 3–4 mice per group; means ± SEM shown. *$P < .05$; **$P < .01$; ***$P < .005$, n.s., not significant, Student *t* test.

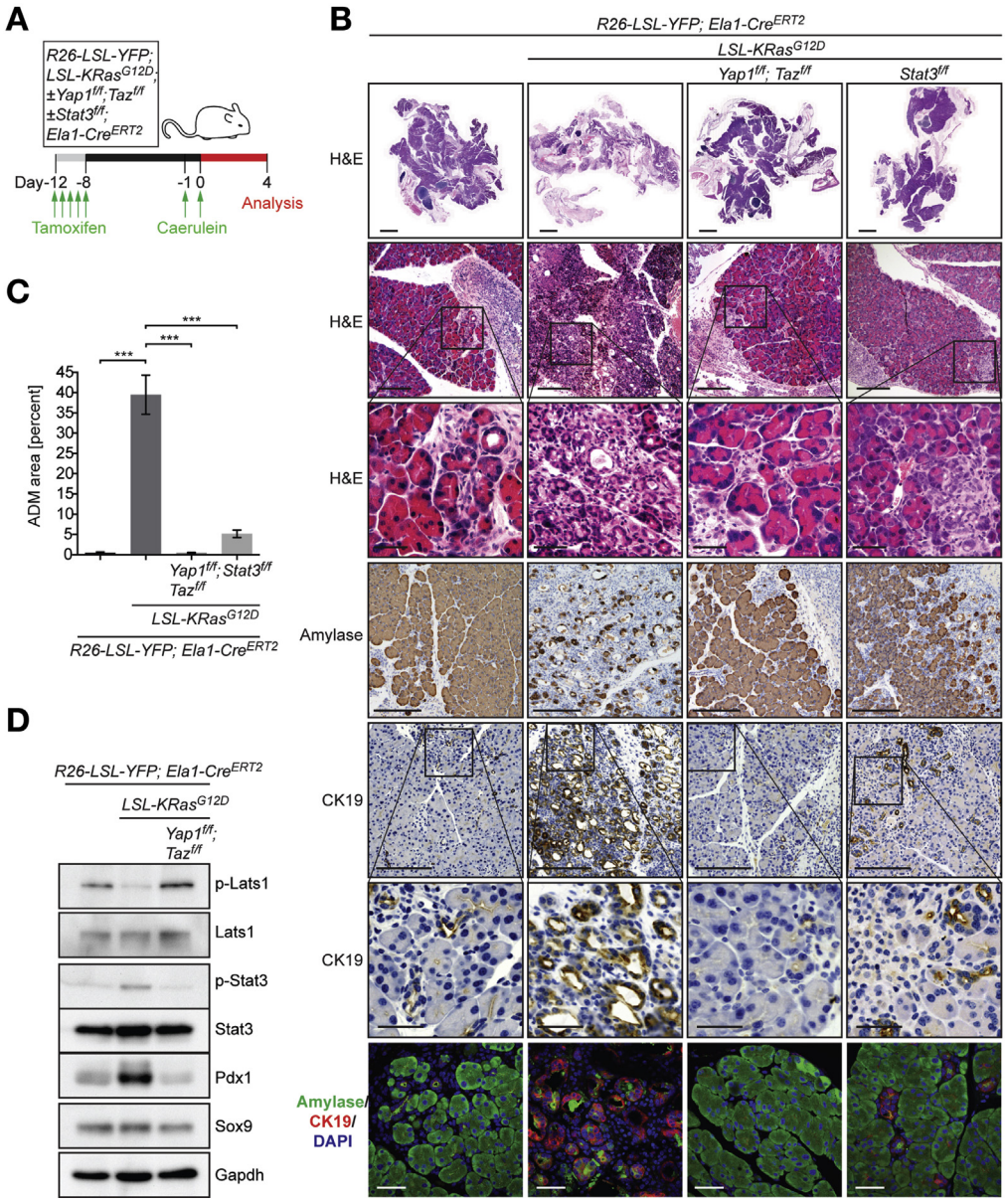


**Figure 5.** YAP1 and TAZ are required for $KRas^{G12D}$-induced ADM in vivo in response to pancreatitis. (*A*) Scheme showing experimental design of caerulein-induced acute pancreatitis in cooperation with acinar-specific $KRas^{G12D}$ mutation. (*B*) H&E stain and amylase and CK19 antibody stains of pancreata from mice of the indicated genotypes. Scale bars: H&E (top row) = 2 mm; (2nd row) = 200 $\mu$m; (3rd row) = 50 $\mu$m; amylase = 200 $\mu$m; CK19 (5th row) = 200 $\mu$m; (6th row) = 50 $\mu$m; double immunofluorescence = 50 $\mu$m. (*C*) Quantification of $CK19^{+}amylase^{+}$ ADM pancreatic area in pancreatic sections of the genotypes shown in (*B*). n = 3 mice per genotype; means ± SEM are shown; $^{***}P < .005$, Student *t* test. (*D*) Immunoblots of pancreas lysates from mice of the indicated genotypes treated as shown in (*A*). DAPI, 4′,6-diamidino-2-phenylindole dihydrochloride.

combination with a GFP lineage tracer (*R26-LSL-YFP*) to allow identification of recombined cells (Figure 3*C*). In this model, GFP-positive acinar cells that had lost both *Yap1* and *Taz* were significantly impaired in caerulein-induced ADM formation (Figure 3*D*), supporting a requirement for YAP1 and TAZ in ADM formation in vivo. Importantly, co-deletion of *Yap1* and *Taz* did not affect acinar cell viability (Supplementary Figure 7*A*).

We next examined the effects of ectopic YAP1/TAZ activation in acinar cells by generating adenoviral vectors encoding constitutively active phosphorylation mutants of YAP1 (Ad-GFP-YAP1-5SA) and TAZ (Ad-GFP-TAZ-S89A) (Supplementary Figure 7*B*–*D*). These mutants are predominantly nuclear and able to induce target gene expression[32,33]: as expected, adenoviral delivery of YAP1-5SA, as well as TAZ-S89A, resulted in up-regulation of their target genes *Ctgf* and *Cyr61* in primary acinar cells (Supplementary Figure 7*E*). Strikingly, acinar explants infected with either Ad-GFP-YAP1-5SA or Ad-GFP-TAZ-S89A, but not Ad-GFP, underwent conversion to a duct cell morphology (Figure 3*E* and *F*). These data suggest that activation of the transcriptional regulators YAP1 and TAZ in acinar cells is sufficient to induce ADM.

## YAP1/TAZ Activation Increases Expression of JAK–STAT3 Pathway Components

To investigate the molecular mechanisms downstream of YAP1/TAZ, we analyzed the published transcription profile of cells overexpressing YAP1.[23] Gene set enrichment analysis of BIOCARTA-annotated pathways in this dataset[34] identified the interleukin (IL)6–JAK–STAT3 signaling cascade as strongly regulated by YAP1 overexpression (Supplementary Figure 8*A*). Importantly, JAK–STAT3 signaling was also

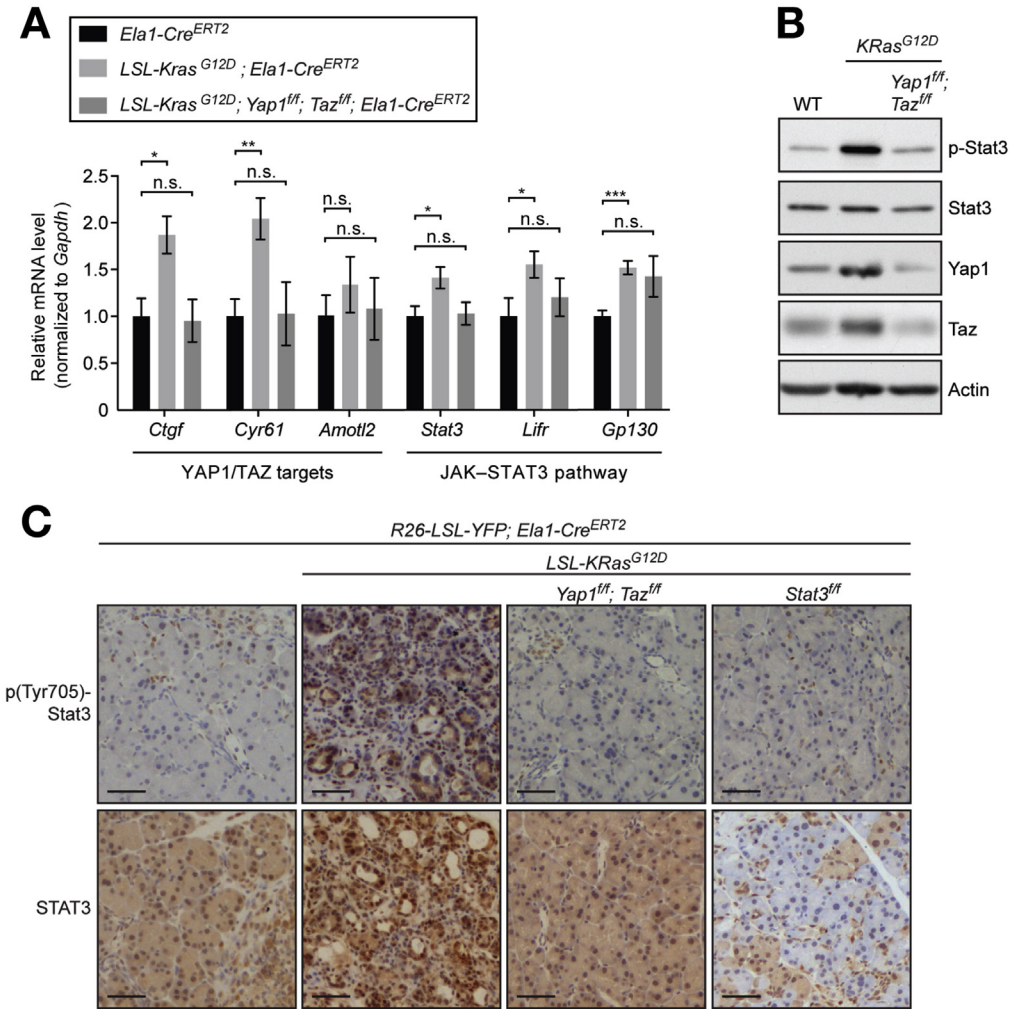


**Figure 6.** *KRas*$^{G12D}$- and caerulein-mediated activation of STAT3 depends on YAP1 and TAZ. (*A*) Quantitative reverse transcription polymerase chain reaction of the YAP1/TAZ target genes *Ctgf*, *Cyr61*, and *Amotl2* and the STAT3 pathway genes *Stat3*, *Lifr*, and *Gp130* in pancreas lysates from *Ela1-Cre*$^{ERT2}$, *LSL-KRas*$^{G12D}$*;Ela1-Cre*$^{ERT2}$ and *LSL-KRas*$^{G12D}$*;Yap1*$^{fl/fl}$*;Taz*$^{fl/fl}$*;Ela1-Cre*$^{ERT2}$ mice 7 days after the last tamoxifen injection. n = 3–5 mice per genotype; means ± SEM are shown; **P* < .05; ***P* < .01; n.s., not significant, Student *t* test. (*B*) Immunoblot analysis of primary acinar cells from wild-type (WT), *LSL-KRas*$^{G12D}$ and *LSL-KRas*$^{G12D}$*;Yap1*$^{fl/fl}$*;Taz*$^{fl/fl}$ mice, 2 days after isolation and infection with Ad-Cre adenovirus. pStat3, phosphorylated Stat3 (Tyr705). (*C*) Immunohistochemistry with antibodies against phosphorylated STAT3 (Tyr705) and STAT3 in pancreata of the indicated genotypes. Mice were treated with tamoxifen and caerulein as indicated in Figure 5*A*. Scale bars = 50 μm. n = 3–5 mice analyzed.



strongly up-regulated in mice with pancreatitis (Supplementary Figure 1*A*), and STAT3 is known to be important for oncogenic *KRas*-induced pancreatic tumor development.[28,29,35] To validate the involvement of this pathway downstream of YAP1/TAZ, we analyzed the expression of JAK–STAT3 pathway components in the human PDAC cell line PANC1, which shows constitutively active YAP1/TAZ (Supplementary Figure 8*B* and *C*). The receptors *LIFR*, *GP130*, *IL13RA1*, and the transcription factor *STAT3* were down-regulated upon *YAP1* and *TAZ* knockdown in PANC1 cells (Figure 4*A*). Accordingly, *YAP1/TAZ* knockdown reduced STAT3 and LIFR protein levels (Figure 4*A* and Supplementary Figure 8*D*). Overexpression of constitutively active YAP1-5SA or TAZ-S89A led to increased protein levels of STAT3 and LIFR in primary mouse acinar cells (Figure 4*B* and Supplementary Figure 9*A* and *B*).

We next tested whether the JAK–STAT3 pathway genes are direct transcriptional targets of the YAP1/TAZ-dependent TEAD transcription factors.[36] The promoter regions of *STAT3*, *LIFR*, and *GP130* contain TEAD4 binding sites, as analyzed by genome-wide ENCODE chromatin immunoprecipitation experiments[37] (Supplementary Figure 9*C*). We confirmed that TEAD4 binding was significantly enriched at the promoters of *STAT3*, *LIFR*, and *GP130* by chromatin immunoprecipitation (Figure 4*C*). In the *STAT3* promoter region, one TEAD consensus binding site GT-IIc[38] was found 312 bp to 306 bp upstream of the *STAT3* transcription start site (Figure 4*D*). We used the entire *STAT3* promoter region including this site in a luciferase reporter construct transfected into the rat pancreatic acinar cell line AR42J. Overexpression of either YAP1-5SA or TAZ-S89A in this cell line significantly increased the luciferase

activity using the *STAT3* promoter construct compared with empty vector control (Figure 4*D*). Mutation of the TEAD binding site abolished the YAP1- and TAZ-induced luciferase activity (Figure 4*D*). Deletion of *Stat3* did not change the expression or protein levels of YAP1 and TAZ in primary acinar cells (Supplementary Figure 10*A*–*C*). Our results suggest that, through TEAD, YAP1 and TAZ regulate the gene expression of the cytokine receptors LIFR and GP130 and the transcription factor STAT3.

## JAK–STAT3 Pathway Activation in Acinar-to-Ductal Metaplasia Lesions

To examine whether JAK–STAT3 signaling is involved in ADM, we analyzed STAT3 activation in response to caerulein-induced pancreatitis. Caerulein treatment led to widespread active, phosphorylated STAT3 (pTyr705-STAT3) in the injured pancreas (Figure 4*E*), in accordance with previous reports.[29] STAT3 phosphorylation and up-regulation of STAT3 and LIFR proteins were also detected in caerulein-treated pancreas lysates (Figure 4*F* and Supplementary Figure 10*D* and *E*), and *Stat3*, *Lifr, Gp130*, and *Jak1* were up-regulated in injured pancreata at the transcriptional level (Figure 4*F*), in agreement with our bioinformatic analysis (Supplementary Figure 1*A*). Co-staining with CK19 and amylase revealed increased staining intensity of STAT3 and LIFR in $KRas^{G12D}$-induced ADM cells in the *Pdx1-Cre* model (Supplementary Figure 11*A* and *B*).

## YAP1/TAZ-Dependent Extreme Acinar-to-Ductal Metaplasia Sensitization by Oncogenic $KRas^{G12D}$

The up-regulation of the JAK–STAT pathway by YAP1/TAZ predicted an increased susceptibility of $KRas^{G12D}$-mutant acinar cells to inflammation, independently of oncogenic transformation. To test this, we challenged control (*R26-LSL-YFP;Ela1-*$Cre^{ERT2}$) and *R26-LSL-YFP;LSL-*$KRas^{G12D}$*;Ela1-*$Cre^{ERT2}$ mice with caerulein to induce pancreatitis (Figure 5*A*). As expected, control mice treated with low doses of caerulein showed acinar cell loss, inflammation, and a limited number of ADM lesions. However, *R26-LSL-YFP;LSL-*$KRas^{G12D}$*;Ela1-*$Cre^{ERT2}$ mice displayed a dramatic increase in ADM lesions double-positive for amylase and CK19 after caerulein treatment, although the recruitment of inflammatory F4/80-positive macrophages was similar to caerulein-treated control mice (Figure 5*B*, *C*, and Supplementary Figure 12*A*). Lineage tracing with the Cre-inducible *R26-LSL-YFP* allele confirmed the acinar cell origin of the ADM lesions (Supplementary Figure 12*B*). Thus, oncogenic Ras mutations dramatically increase the susceptibility of acinar cells to undergo ADM, possibly by increasing acinar cell sensitivity to inflammatory cytokines through up-regulation of *Stat3*, *Lifr*, and *Gp130*.

We next tested the significance of YAP1/TAZ and STAT3 in Ras-induced ADM sensitization directly. Strikingly, co-deletion of *Yap1* and *Taz* completely blocked the enhanced formation of these pancreatitis-induced ADM lesions by $KRas^{G12D}$ (Figure 5*B* and *C*). Pancreata of *R26-LSL-YFP;LSL-*$KRas^{G12D}$*;*$Yap1^{fl/fl}$*;*$Taz^{fl/fl}$*;Ela1-*$Cre^{ERT2}$ mice showed normal morphology with some signs of caerulein-induced acinar cell loss and inflammation similar to the extent observed in control mice (Figure 5*B* and Supplementary Figure 12*A*). Additionally, in agreement with previous results,[29] loss of STAT3 significantly reduced caerulein-induced CK19-positive ductal structures in the mutant $KRas^{G12D}$ background (Figure 5*B* and *C*). Ras-induced ADM formation resulted in increased expression of the pancreatic progenitor marker Pdx1 and the duct marker Sox9, which was dependent on YAP1/TAZ (Figure 5*D* and Supplementary Figure 13*A*). These results suggest that expression of $KRas^{G12D}$ in normal, untransformed acinar cells results in extreme sensitization to pancreatitis-induced ADM, which is mediated by YAP1/TAZ and STAT3.

## JAK–STAT3 Pathway Acts Downstream of YAP1/TAZ in Response to Oncogenic Ras and Inflammatory Stimuli

We next addressed the function of YAP1/TAZ and JAK-STAT3 signaling as effectors of oncogenic Ras. $KRas^{G12D}$ was activated in adult acinar cells using tamoxifen-inducible *LSL-*$KRas^{G12D}$*;Ela1-*$Cre^{ERT2}$ mice, and gene expression was analyzed 7 days later, when pancreas histology was unaltered and no tumor initiation had occurred. $KRas^{G12D}$ activation in normal untransformed acinar cells resulted in increased expression of the YAP1/TAZ target genes *Ctgf* and *Cyr61*, accompanied by transcriptional induction of *Stat3*, *Lifr*, and *Gp130* (Figure 6*A*). Importantly, activation of STAT3 pathway genes by oncogenic $KRas^{G12D}$ in this context occurred without caerulein treatment. After deletion of $Yap1^{fl/fl}$;$Taz^{fl/fl}$, $KRas^{G12D}$ was unable to induce YAP1/TAZ target genes or *Stat3*, *Lifr*, and *Gp130* expression (Figure 6*A*). $KRas^{G12D}$ activation in primary acinar cells in vitro increased YAP1 and TAZ protein levels, STAT3 protein levels and STAT3 phosphorylation (Figure 6*B* and Supplementary Figure 13*B*), but deletion of $Yap1^{fl/fl}$;$Taz^{fl/fl}$ modestly reduced STAT3 protein levels and greatly impaired the $KRas^{G12D}$-induced phosphorylation of STAT3 in acinar cells in vitro (Figure 6*B* and Supplementary Figure 13*B*). In agreement with these results, caerulein treatment of tamoxifen-induced *LSL-*$KRas^{G12D}$*;Ela1-*$Cre^{ERT2}$ mice led to a dramatic increase in STAT3 phosphorylation at tyrosine 705, which was completely abolished in the absence of YAP1 and TAZ (Figure 6*C*, Figure 5*D*, and Supplementary Figure 13*A*). YAP1 and TAZ deletion also diminished the caerulein-induced phosphorylation of STAT3 in pancreatic acinar cells wild type for *KRas* (Supplementary Figure 14*A* and *B*). These data indicate that, even in the absence of an inflammatory stimulus or tumorigenesis, oncogenic Ras mutation leads to YAP1/TAZ and JAK–STAT3 pathway activation, and YAP1 and TAZ act upstream of the JAK-STAT3 signaling pathway in oncogenic KRas-induced ADM.

## Deletion of YAP1 and TAZ Reduces Inflammation-Induced Ras Activation

Inflammatory insults lead to hyperstimulation of oncogenic Ras activity, and interfering with the inflammatory signaling cascade interrupts this feedback activation.[18] We next tested whether YAP1/TAZ affects oncogenic Ras activity.

Caerulein treatment increased Ras activity in mice expressing *KRas*$^{G12D}$ in acinar cells (Supplementary Figure 15*A* and *B*), as shown previously.[18] Deletion of *Yap1* and *Taz* in the *KRas*$^{G12D}$ background reduced Ras activation after caerulein treatment (Supplementary Figure 15*A* and *B*). Overexpression of constitutively active YAP1 in primary acinar cells increased

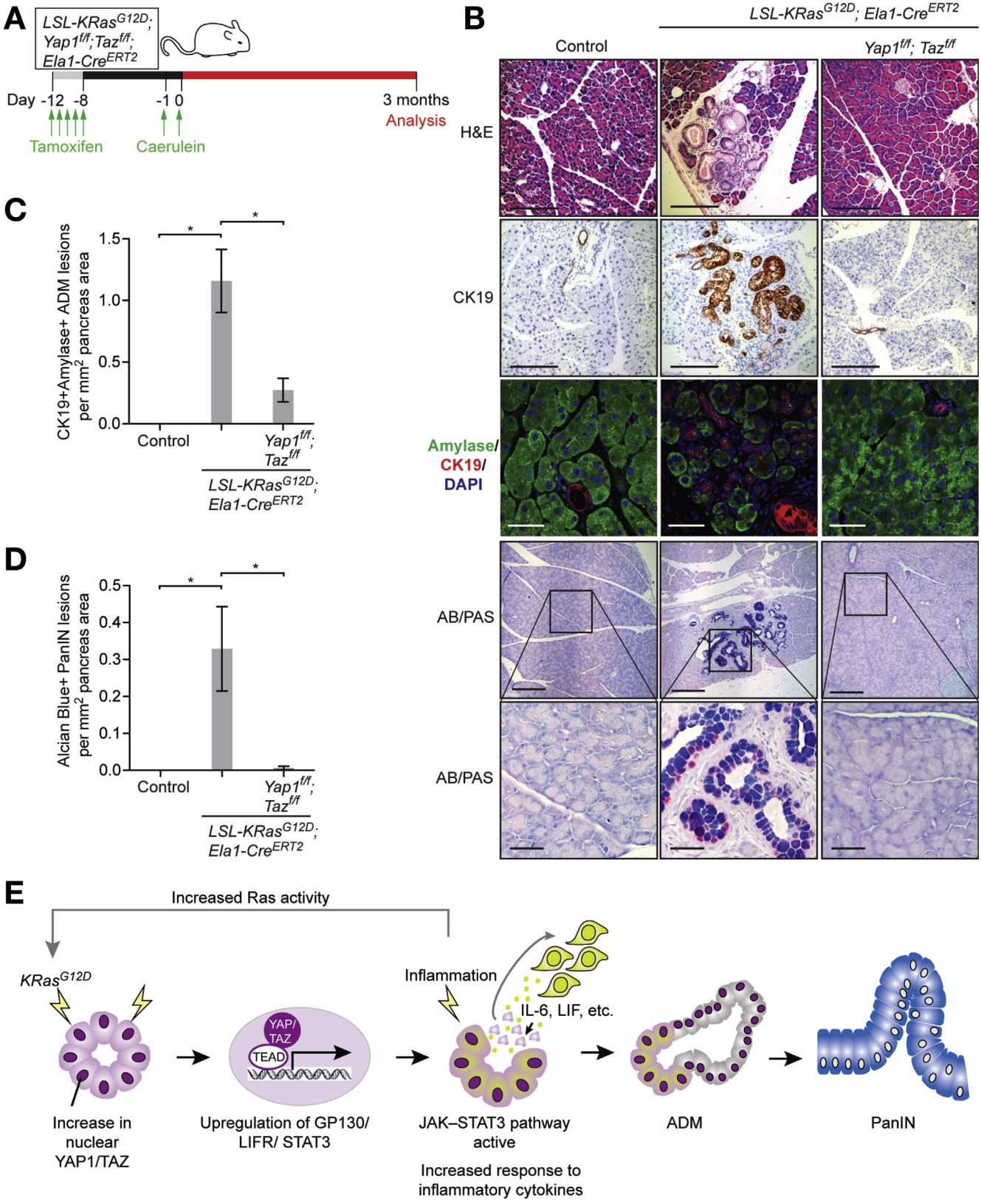

Ras activity (Supplementary Figure 15*C*). Hyperactivating oncogenic Ras by TGFα resulted in a more efficient differentiation of acinar to duct cells in vitro[39] (Supplementary Figure 16*A* and *B*). However, YAP1 and TAZ were required for $KRas^{G12D}$-induced ADM, even in the presence of TGFα (Supplementary Figure 16*A* and *B*).

### *YAP1 and TAZ Are Required for* $KRas^{G12D}$*-Induced Pancreatic Intraepithelial Neoplasia Formation*

To determine whether the block to ADM in $Yap1^{fl/fl}$;$Taz^{fl/fl}$;*LSL-*$KRas^{G12D}$;*Ela1-*$Cre^{ERT2}$ mice affects the development of pancreatic cancer, we assessed PanIN lesions 3 months after the transient induction of pancreatitis by caerulein (Figure 7*A*). At this stage, *LSL-*$KRas^{G12D}$;*Ela1-*$Cre^{ERT2}$ mice displayed CK19/amylase double-positive ADM lesions and CK19- and AB/PAS-positive PanIN lesions (Figure 7*B–D*). *Yap1* and *Taz* co-deletion resulted in a striking decrease in ADM lesions and these mice were free of PanIN lesions, similar to control mice (Figure 7*B–D*). These results show that acinar cell-specific YAP1/TAZ signaling is essential for oncogenic $KRas^{G12D}$-induced PanIN formation in the context of pancreatitis, and that STAT3 signaling appears to be a critical downstream factor in this process.

## Discussion

Acinar-to-ductal reprogramming is now established as an important precursor to PanIN lesions and progression to pancreatic cancer, but the molecular mechanisms that drive this process have remained unclear. Our results confirm that $KRas^{G12D}$ mutation synergizes with inflammatory insults to induce widespread and persistent ADM lesions, and we elucidate how this synergy occurs (Figure 7*E*). We find that the transcriptional regulators YAP1 and TAZ are required for $KRas^{G12D}$ to promote acinar-to-ductal reprogramming, both in vitro and in vivo. In the absence of YAP1 and TAZ, $KRas^{G12D}$ is unable to induce PanIN lesions, suggesting that acinar-to-ductal reprogramming via YAP1/TAZ is an obligate step in pancreatic cancer initiation from acinar cells.

Mechanistically, active YAP1 and TAZ interact with the transcription factor TEAD, which binds and up-regulates the expression of several genes in the JAK–STAT3 pathway. This pathway controls the response to inflammatory cytokines like IL6, which is secreted during caerulein-induced pancreatitis and also present at high levels in pancreatic tumors, promoting PanIN progression in $KRas^{G12D}$ mice.[35,40] A recent study found that the IL6 co-receptor GP130, up-regulated by YAP1/TAZ in our study, also activates YAP1 independently of STAT3.[41] Additionally, LIFR has been shown to act upstream of YAP1 signaling.[42] This would create a positive feedback loop amplifying YAP1 activity.

Our data in mouse models expressing $KRas^{G12D}$ are consistent with findings in cultured cells showing that Ras signaling both stabilizes and activates YAP1.[43,44] Recent studies have implicated YAP1 as an important driver of pancreatic cancer progression at later stages in collaboration with oncogenic Ras, and as a mechanism of escape from Ras-RAF-MEK-targeted therapies.[19,20,45] However, data from patient samples has shown that the incidence of *KRas* codon 12 mutations is already >90%, even in the earliest pre-neoplastic lesions.[8] Here we show that YAP1 acts downstream of oncogenic Ras at this early reprogramming stage. There is likely redundancy between YAP1 and TAZ because co-deletion of *Yap1* and *Taz* is more efficient in blocking $KRas^{G12D}$- induced ADM in the in vitro assay compared with either single mutant. YAP1 seems able to compensate for TAZ deletion but not vice versa, however, overexpression of constitutively active YAP1 or TAZ alone is sufficient to induce ADM.

We noted that inactivation of YAP1 and TAZ reduced ADM formation more efficiently than *Stat3* deletion (Figure 5). It has been shown that the Hippo pathway also interacts with other signaling pathways that have implications in ADM, such as Wnt and Notch pathways.[23,46] YAP1/TAZ-dependent regulation of these pathways might also contribute to ADM formation.

The presence of the $KRas^{G12D}$ mutation in ADM cells in an inflammatory microenvironment is known to be sufficient for progression to PanIN lesions and pancreatic cancer.[1] Additionally, inflammation in the pancreas creates a feedback loop leading to hyperactivation of oncogenic $KRas^{G12D}$ (Figure 7*E*).[18] The $KRas^{G12D}$ mutation and subsequent hyperactivation promotes pancreatic cancer at 2 levels: it creates a susceptible "cell of origin" by inducing acinar-to-ductal reprogramming; and it also acts as the transforming driver that enables progression toward malignancy. This model explains why *KRas* mutations in pancreatic cancer are so common, and why they frequently appear very early, as a gatekeeper mutation, in pancreatic acinar cells.

## Supplementary Material

Note: To access the supplementary material accompanying this article, visit the online version of *Gastroenterology* at www.gastrojournal.org, and at http://dx.doi.org/10.1053/j.gastro.2016.05.006.

**Figure 7.** YAP1 and TAZ are required for $KRas^{G12D}$-induced PanIN. (*A*) Scheme showing experimental design of caerulein-induced PanIN formation in the $KRas^{G12D}$ background. (*B*) H&E, amylase, and CK19 antibody, and Alcian Blue/periodic acid–Schiff (AB/PAS) stains of pancreata from mice of the indicated genotypes. Scale bars: H&E = 200 μm; CK19 = 200 μm; double immunofluorescence = 50 μm; AB/PAS (4th row) = 200 μm; AB/PAS (5th row) = 50 μm. (*C*) Quantification of $CK19^{+}amylase^{+}$ ADM lesions in control, *LSL-*$KRas^{G12D}$;*Ela1-*$Cre^{ERT2}$ and *LSL-*$KRas^{G12D}$;$Yap1^{fl/fl}$;$Taz^{fl/fl}$;*Ela1-*$Cre^{ERT2}$ mice. n = 3–4 mice per genotype; means ± SEM are shown; $^{*}P < .05$, Student *t* test. (*D*) Quantification of AB/PAS-positive PanIN lesions in control, *LSL-*$KRas^{G12D}$;*Ela1-*$Cre^{ERT2}$, and *LSL-*$KRas^{G12D}$;$Yap1^{fl/fl}$;$Taz^{fl/fl}$;*Ela1-*$Cre^{ERT2}$ mice. n = 3–4 mice per group; means ± SEM are shown; $^{*}P < .05$, Student *t* test. (*E*) Scheme showing the roles of YAP1 and TAZ in pancreatic cancer initiation by inducing ADM in response to oncogenic $KRas^{G12D}$ and inflammation. See text for details.

## References


1. Guerra C, Schuhmacher AJ, Canamero M, et al. Chronic pancreatitis is essential for induction of pancreatic ductal adenocarcinoma by K-Ras oncogenes in adult mice. Cancer Cell 2007;11:291–302.
2. Jensen JN, Cameron E, Garay MV, et al. Recapitulation of elements of embryonic development in adult mouse pancreatic regeneration. Gastroenterology 2005; 128:728–741.
3. Means AL, Meszoely IM, Suzuki K, et al. Pancreatic epithelial plasticity mediated by acinar cell transdifferentiation and generation of nestin-positive intermediates. Development 2005;132:3767–3776.
4. Reichert M, Rustgi AK. Pancreatic ductal cells in development, regeneration, and neoplasia. J Clin Invest 2011; 121:4572–4578.
5. Hruban RH, Adsay NV, Albores-Saavedra J, et al. Pancreatic intraepithelial neoplasia: a new nomenclature and classification system for pancreatic duct lesions. Am J Surg Pathol 2001;25:579–586.
6. Biankin AV, Waddell N, Kassahn KS, et al. Pancreatic cancer genomes reveal aberrations in axon guidance pathway genes. Nature 2012;491:399–405.
7. DiGiuseppe JA, Hruban RH, Offerhaus GJ, et al. Detection of K-ras mutations in mucinous pancreatic duct hyperplasia from a patient with a family history of pancreatic carcinoma. Am J Pathol 1994;144:889–895.
8. Kanda M, Matthaei H, Wu J, et al. Presence of somatic mutations in most early-stage pancreatic intraepithelial neoplasia. Gastroenterology 2012;142:730–733 e9.
9. Eser S, Schnieke A, Schneider G, et al. Oncogenic KRAS signalling in pancreatic cancer. Br J Cancer 2014; 111:817–822.
10. Bardeesy N, DePinho RA. Pancreatic cancer biology and genetics. Nat Rev Cancer 2002;2:897–909.
11. Carriere C, Young AL, Gunn JR, et al. Acute pancreatitis markedly accelerates pancreatic cancer progression in mice expressing oncogenic Kras. Biochem Biophys Res Commun 2009;382:561–565.
12. Hofbauer B, Saluja AK, Lerch MM, et al. Intra-acinar cell activation of trypsinogen during caerulein-induced pancreatitis in rats. Am J Physiol 1998; 275:G352–G362.
13. Morris JPt, Cano DA, Sekine S, et al. Beta-catenin blocks Kras-dependent reprogramming of acini into pancreatic cancer precursor lesions in mice. J Clin Invest 2010; 120:508–520.
14. **Shi G, DiRenzo D, Qu C**, et al. Maintenance of acinar cell organization is critical to preventing Kras-induced acinar-ductal metaplasia. Oncogene 2013;32:1950–1958.
15. Ji B, Tsou L, Wang H, et al. Ras activity levels control the development of pancreatic diseases. Gastroenterology 2009;137:1072–1082; 1082 e1–e6.
16. Hingorani SR, Wang L, Multani AS, et al. Trp53R172H and KrasG12D cooperate to promote chromosomal instability and widely metastatic pancreatic ductal adenocarcinoma in mice. Cancer Cell 2005;7:469–483.
17. Siveke JT, Einwachter H, Sipos B, et al. Concomitant pancreatic activation of Kras(G12D) and Tgfa results in cystic papillary neoplasms reminiscent of human IPMN. Cancer Cell 2007;12:266–279.
18. Daniluk J, Liu Y, Deng D, et al. An NF-kappaB pathway-mediated positive feedback loop amplifies Ras activity to pathological levels in mice. J Clin Invest 2012; 122:1519–1528.
19. **Kapoor A, Yao W, Ying H**, et al. Yap1 activation enables bypass of oncogenic Kras addiction in pancreatic cancer. Cell 2014;158:185–197.
20. Zhang W, Nandakumar N, Shi Y, et al. Downstream of mutant KRAS, the transcription regulator YAP is essential for neoplastic progression to pancreatic ductal adenocarcinoma. Sci Signal 2014;7:ra42.
21. Kranz A, Fu J, Duerschke K, et al. An improved Flp deleter mouse in C57Bl/6 based on Flpo recombinase. Genesis 2010;48:512–520.
22. Ulmasov B, Oshima K, Rodriguez MG, et al. Differences in the degree of cerulein-induced chronic pancreatitis in C57BL/6 mouse substrains lead to new insights in identification of potential risk factors in the development of chronic pancreatitis. Am J Pathol 2013;183:692–708.
23. **Yimlamai D, Christodoulou C**, Galli GG, et al. Hippo pathway activity influences liver cell fate. Cell 2014; 157:1324–1338.
24. He TC, Zhou S, da Costa LT, et al. A simplified system for generating recombinant adenoviruses. Proc Natl Acad Sci U S A 1998;95:2509–2514.
25. Gruber R, Zhou Z, Sukchev M, et al. MCPH1 regulates the neuroprogenitor division mode by coupling the centrosomal cycle with mitotic entry through the Chk1-Cdc25 pathway. Nat Cell Biol 2011;13:1325–1334.
26. **Subramanian A, Tamayo P**, Mootha VK, et al. Gene set enrichment analysis: a knowledge-based approach for interpreting genome-wide expression profiles. Proc Natl Acad Sci U S A 2005;102:15545–15550.
27. Miyamoto Y, Maitra A, Ghosh B, et al. Notch mediates TGF alpha-induced changes in epithelial differentiation during pancreatic tumorigenesis. Cancer Cell 2003; 3:565–576.
28. Corcoran RB, Contino G, Deshpande V, et al. STAT3 plays a critical role in KRAS-induced pancreatic tumorigenesis. Cancer Res 2011;71:5020–5029.
29. **Fukuda A, Wang SC**, Morris JPt, et al. Stat3 and MMP7 contribute to pancreatic ductal adenocarcinoma initiation and progression. Cancer Cell 2011;19:441–455.
30. George NM, Day CE, Boerner BP, et al. Hippo signaling regulates pancreas development through inactivation of Yap. Mol Cell Biol 2012;32:5116–5128.
31. Hingorani SR, Petricoin EF, Maitra A, et al. Preinvasive and invasive ductal pancreatic cancer and its early detection in the mouse. Cancer Cell 2003;4:437–450.
32. Zhao B, Wei X, Li W, et al. Inactivation of YAP oncoprotein by the Hippo pathway is involved in cell contact inhibition and tissue growth control. Genes Dev 2007; 21:2747–2761.
33. Lei QY, Zhang H, Zhao B, et al. TAZ promotes cell proliferation and epithelial-mesenchymal transition and is inhibited by the hippo pathway. Mol Cell Biol 2008; 28:2426–2436.

34. **Huang DW, Sherman BT**, Lempicki RA. Systematic and integrative analysis of large gene lists using DAVID bioinformatics resources. Nat Protoc 2009;4:44–57.
35. Lesina M, Kurkowski MU, Ludes K, et al. Stat3/Socs3 activation by IL-6 transsignaling promotes progression of pancreatic intraepithelial neoplasia and development of pancreatic cancer. Cancer Cell 2011;19:456–469.
36. Mahoney WM Jr, Hong JH, Yaffe MB, et al. The transcriptional co-activator TAZ interacts differentially with transcriptional enhancer factor-1 (TEF-1) family members. Biochem J 2005;388:217–225.
37. ENCODE Project Consortium. An integrated encyclopedia of DNA elements in the human genome. Nature 2012;489:57–74.
38. Home P, Saha B, Ray S, et al. Altered subcellular localization of transcription factor TEAD4 regulates first mammalian cell lineage commitment. Proc Natl Acad Sci U S A 2012;109:7362–7367.
39. **Eser S, Reiff N, Messer M**, et al. Selective requirement of PI3K/PDK1 signaling for Kras oncogene-driven pancreatic cell plasticity and cancer. Cancer Cell 2013;23:406–420.
40. Suzuki S, Miyasaka K, Jimi A, et al. Induction of acute pancreatitis by cerulein in human IL-6 gene transgenic mice. Pancreas 2000;21:86–92.
41. Taniguchi K, Wu LW, Grivennikov SI, et al. A gp130-Src-YAP module links inflammation to epithelial regeneration. Nature 2015;519:57–62.
42. Chen D, Sun Y, Wei Y, et al. LIFR is a breast cancer metastasis suppressor upstream of the Hippo-YAP pathway and a prognostic marker. Nat Med 2012;18:1511–1517.
43. **Hong X, Nguyen HT**, Chen Q, et al. Opposing activities of the Ras and Hippo pathways converge on regulation of YAP protein turnover. EMBO J 2014;33:2447–2457.
44. Reddy BV, Irvine KD. Regulation of Hippo signaling by EGFR-MAPK signaling through Ajuba family proteins. Dev Cell 2013;24:459–471.
45. Lin L, Sabnis AJ, Chan E, et al. The Hippo effector YAP promotes resistance to RAF- and MEK-targeted cancer therapies. Nat Genet 2015;47:250–256.
46. Azzolin L, Panciera T, Soligo S, et al. YAP/TAZ incorporation in the beta-catenin destruction complex orchestrates the Wnt response. Cell 2014;158:157–170.
47. Cordenonsi M, Zanconato F, Azzolin L, et al. The Hippo transducer TAZ confers cancer stem cell-related traits on breast cancer cells. Cell 2011;147:759–772.

**Author names in bold designate shared co-first authorship.**

**Received December 24, 2015. Accepted May 14, 2016.**

**Reprint requests**
Address requests for reprints to: Axel Behrens, PhD, Mammalian Genetics Laboratory, The Francis Crick Institute, Lincoln's Inn Fields Laboratory, 44 Lincoln's Inn Fields, London WC2A 3LY, UK. e-mail: Axel.Behrens@crick.ac.uk; fax: (44) 207 269 3581.

**Acknowledgments**
H. Gerhardt kindly provided *Yap1*$^{fl/fl}$ mice and S. Piccolo kindly provided YAP1 (5SA) and TAZ (S89A) vectors. The authors thank C. Cremona and N. Tapon for comments on the manuscript and P. Chakravarty of the Francis Crick Institute Bioinformatics facility for help with gene set enrichment analysis.

Author contributions: RG conceived and designed the study, performed experiments, analyzed data, and wrote the manuscript; RP assisted with in vitro ADM assay; EN and BS-D performed immunohistochemistry; GS provided histopathology analysis; AB supervised the study and wrote the manuscript.

**Conflicts of interest**
The authors disclose no conflicts.

**Funding**
This study was supported by the Francis Crick Institute, which receives its core funding from Cancer Research UK, the UK Medical Research Council, and the Wellcome Trust. Ralph Gruber was funded by an EMBO Long-Term Fellowship and a Cancer Research UK postdoctoral fellowship.